Journal of Alloys and Compounds 480 (2009) 259–264

Contents lists available at ScienceDirect

Journal of Alloys and Compounds

journal homepage: www.elsevier.com/locate/jallcom

Composition of electrodeposited Zn–Cr alloy coatings and phase transformations induced by thermal treatment

Tz. Boiadjieva[a], K. Petrov[b], H. Kronberger[c], A. Tomandl[d], G. Avdeev[e], W. Artner[a], T. Lavric[f], M. Monev[e,*]

[a] Centre of Electrochemical Surface Technology GmbH, Viktor-Kaplan-Straße 2, 2700 Wiener Neustadt, Austria
[b] Institute of General and Inorganic Chemistry, Bulg. Acad. Sci., Acad. G. Bonchev Str., bl. 11, 1113 Sofia, Bulgaria
[c] TU-Vienna, Institute for Chemical Technology and Analytics, Getreidemarkt 9/164ec, A-1060 Vienna, Austria
[d] voestalpine Stahl GmbH, Voestalpine-Strasse 3, 4020 Linz, Austria
[e] Institute of Physical Chemistry, Bulg. Acad. Sci., Acad. G. Bonchev Str., bl. 11, 1113 Sofia, Bulgaria
[f] Andritz AG, Eibesbrunnergasse 20, A-1121 Vienna, Austria

ARTICLE INFO

Article history:
Received 14 November 2008
Received in revised form 23 January 2009
Accepted 8 February 2009
Available online 21 February 2009

Keywords:
Zn–Cr alloy coatings
Electrodeposition
Annealing
Phase composition
Phase transformations
X-ray diffraction

ABSTRACT

Zn–Cr alloy coatings were obtained in a flow cell, for modeling the process of high speed electrodeposition on steel strips. Alloy coatings, containing between 6 and 18 at.% Cr were annealed at 260 °C in an inert atmosphere. The phase composition and the crystallographic characteristics of "as prepared" and "annealed" coatings, were studied by XRD. It is shown that non-equilibrium δ- and Γ-(Zn,Cr) phases are major constituents of the "as prepared" coatings. On annealing, equilibrium ζ-$CrZn_{13}$ phase precipitates from δ- and Γ-supersaturated solid solutions. The lattice parameters and the similarities in phase composition of the annealed coatings, deposited onto two types of substrates – low carbon steel and Cr plated (protected) low carbon steel – show that if Fe from the substrate "contaminates" the precipitated ζ-$CrZn_{13}$ phases, its relative amount do not exceed few tenths of a percent.

The influence of the elemental composition, conditions of electrochemical deposition, and post-deposition thermal treatment on phase composition of the coatings is discussed.

1. Introduction

Zn–Cr alloy coatings are of interest due to their higher corrosion protective ability, at reduced thickness, in comparison to that of pure Zn coatings [1–3]. Corrosion protective properties of the coatings – resistance to surface rusting, chipping resistance, corrosion resistance after working, resistance to pitting corrosion – are closely related to their phase composition [4]. Several important characteristics, such as formability [4], adhesion to the substrate [5,6] and hardness [3] have been associated with the crystal structure and spatial distribution of phases within the coating.

Solid Cr has a low solubility in liquid Zn which makes it difficult to obtain even low-Cr-alloys [7]. That is why the Cr–Zn equilibrium phase diagram has been evaluated mainly for its Zn-rich part, where two inter-metallic compounds—θ-$CrZn_{17}$ and ζ-$CrZn_{13}$ have been reported. The hexagonal θ-$CrZn_{17}$ (a = 12.89–12.92 Å; c = 30.5–30.56 Å) crystallizes with 3.8–7 mass% Cr [8–11]. The existence of monoclinic ζ-$CrZn_{13}$ has been reported by Hartman et al. [12]. Later, Brown suggested that ζ-$CrZn_{13}$ is probably isotypic with several ζ-MZn_{13} (M = Co, Fe, Mn) phases [13]. To our knowledge, complete structure analysis of ζ-$CrZn_{13}$ has not been performed so far. Studies of the Zn-rich corner of the Fe–Zn–Cr system, carried out recently, brought evidence that minor Fe impurities promote formation of ζ-phase [11,14].

Recent trends in elaboration and characterization of alloyed zinc protective coatings are focused on methods of deposition at non-equilibrium conditions, like physical vapor deposition and electrodeposition. In some cases, these methods allow preparation of thin coatings which phase composition is unattainable by other conventional methods. They are adaptable to continuous operational mode and allow high deposition rate.

In electrodeposited [15–17] and physically vapor deposited [3] Zn–Cr coatings, several unidentified non-equilibrium Zn–Cr phases have been found. Detailed analyses have shown that the phase composition of the coatings depends on both deposition conditions and Cr atomic fraction [6,18–20]. With increasing Cr content the phase composition changes in the sequence: hexagonal η-(Zn,Cr) → hexagonal δ-(Zn,Cr) → cubic Γ-(Zn,Cr), including concentration intervals in which two or all the three phases coexist [3,4,6,19,20]. In some studies, the hexagonal (hcp) η-(Zn,Cr) variable-composition phase is regarded as a phase of the equilibrium phase diagram [6,19]. The non-equilibrium Zn–Cr phase

* Corresponding author. Tel: +359 2 979 25 38; fax: +359 2 873 49 68.
E-mail address: monev@ipc.bas.bg (M. Monev).

0925-8388/$ – see front matter © 2009 Elsevier B.V. All rights reserved.
doi:10.1016/j.jallcom.2009.02.026

diagram has not been extensively studied. The available data however, indicate that δ- and Γ-phases may be regarded as non-equilibrium, super-saturated solid solutions. When annealed at relatively low temperatures (170–225 °C), the δ-phase transforms to a mixture of phases (ζ + δ) or a single phase (ζ), depending on temperature and Cr content, while the Γ-phase is stable up to at least 275 °C [6]. In other words, the phase composition of the coating could be properly controlled by varying the conditions of deposition and annealing.

A potential user of the Zn–Cr alloy coatings is the automotive industry [1,2]. Therefore, in order to reach the working conditions of the high speed electrodeposition on steel strips, a flow cell, for preparation of Zn–Cr alloy coatings was used in the present study. The phase composition of the "as prepared" alloy coatings and the phase transformations caused by annealing of these coatings were investigated. For evaluation of a possible influence of Fe from the substrate on both: phase formation and thermal transformation of the non-equilibrium phases, alloy coatings with different Cr content were deposited on "raw" and on Cr-"protected" steel strips.

2. Experimental

Zn–Cr alloy coatings with Cr content between 6 and 18 at.% were electrodeposited from an electrolyte, containing 40 g l^{-1} Zn, 15 g l^{-1} Cr (added as sulphates) and polyethyleneglycol (1 g l^{-1}), pH 2.0, adjusted with sulphuric acid, in a 20 l flow cell, flow rate 4 m s^{-1}, current density (c.d.) within the 80–120 A dm^{-2} range, electrolyte temperature 40 °C onto low carbon steel substrates with dimensions 115 mm × 85 mm. The Zn–Cr coatings are relatively thin having a thickness of about 3.0–3.5 μm.

In order to avoid a possible influence of Fe contamination on the formation of ζ-(Zn,Cr) phase, experiments were carried out on "raw" steel strips as well as on steel strips preliminarily coated with a protective Cr layer. Further on, these samples are denoted as Fe/Zn–Cr and Fe/Cr/Zn–Cr, respectively. The Cr layer (thickness of 4 μm) onto the steel substrates was electrodeposited from conventional Cr(VI) electrolyte (150 g l^{-1} CrO_3), c.d. 100 A dm^{-2}, electrolyte temperature 35 °C. Ti/IrO_x was used as an anode.

The Zn–Cr alloy coatings, deposited onto steel and Cr coated steel substrates were annealed in an inert atmosphere (95% N_2, 5% H_2) at 260 °C for 90 min.

The Cr content in the alloy coatings was determined using fluorescence X-ray analysis (FXRA) (Fischerscope XDL-B, Software WinFTM 6.09). Values for alloy coatings thickness were obtained from FXRA as well.

X-ray diffraction (XRD) measurements were performed on a Stoe automatic powder diffractometer with strictly monochromated Cu $K\alpha_1$ radiation. The XRD patterns for the thin Zn–Cr galvanic coatings on steel and Cr-coated steel substrates, as-deposited and after thermal treatment, were recorded in grazing incidence X-ray diffraction (GIXD) geometry at two constant incident angles of 3° and 5°. In this geometry, the diffraction patterns provide primarily information about phase composition of the coating with a minimum diffraction contribution from the substrate. In order to check for presence of preferred orientation effects, the XRD powder patterns were recorded at two mutually perpendicular lateral directions.

Indexing, determination of unit cell parameters and evaluation of volume fraction of phase constituents were carried out after least-squares procedure of profile fitting, performed with the PowderCell software package [21].

3. Results and discussion

Typical XRD patterns for the "as prepared" and thermally treated Fe/Zn–Cr and Fe/Cr/Zn–Cr galvanic coatings on steel and Cr coated steel substrates are presented in Figs. 1–4. Phase composition and unit cell parameters data are summarized in Table 1.

The analyzed XRD patterns contain lines of the following main phases:

α-Fe—Body centered cubic (bcc) lattice, space group Im-3m (Nr. 229), a = 2.865 Å. The lattice parameter of this phase remains constant with changes in the nominal composition of the coating. The presence of its peaks in the patterns is due to diffraction from the substrates. Hence, these peaks were not taken into account when calculating the relative phase composition of the coatings. Their angular positions, however, were used as reference in calculating the lattice parameters of the remaining phases.

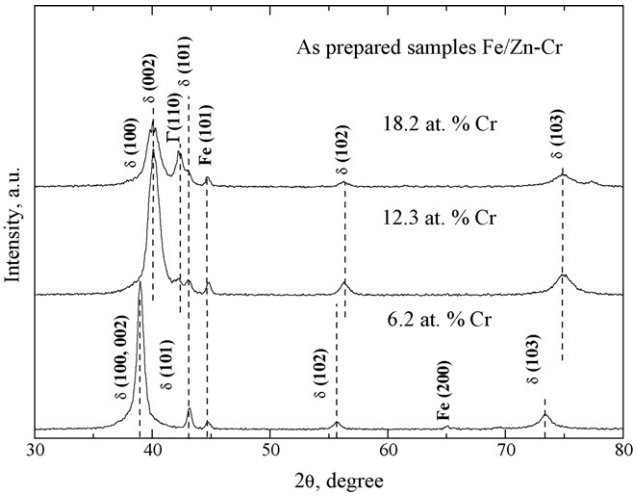

Fig. 1. XRD patterns of "as prepared" Fe/Zn–Cr samples.

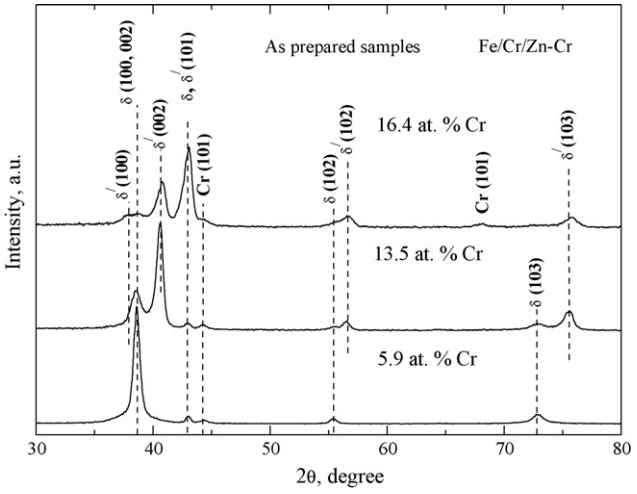

Fig. 2. XRD patterns of "as prepared" Fe/Cr/Zn–Cr samples.

α-Cr—Body centered cubic (bcc) lattice, space group Im-3m (Nr. 229), a = 2.885 Å; unit cell volume V = 24.012 $Å^3$. This phase is observed in substrates coated preliminary with protective Cr-layer. η-Zn—Hexagonal lattice, distorted hexagonal close packing (hcp) of Zn atoms, space group $P6_3/mmc$ (Nr. 194), a = 2.665 Å;

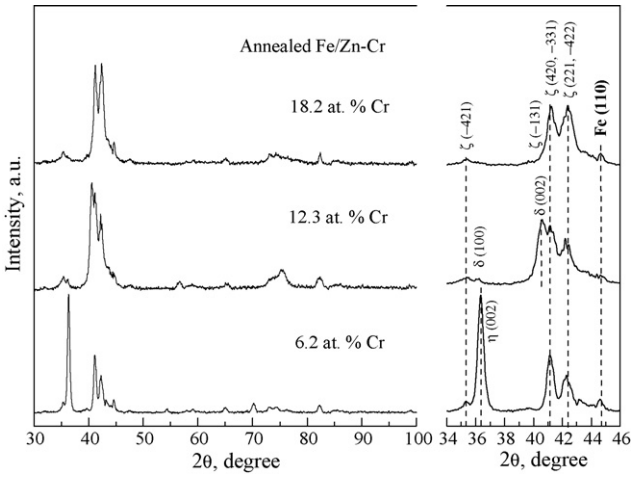

Fig. 3. XRD patterns of "annealed" Fe/Zn–Cr samples.

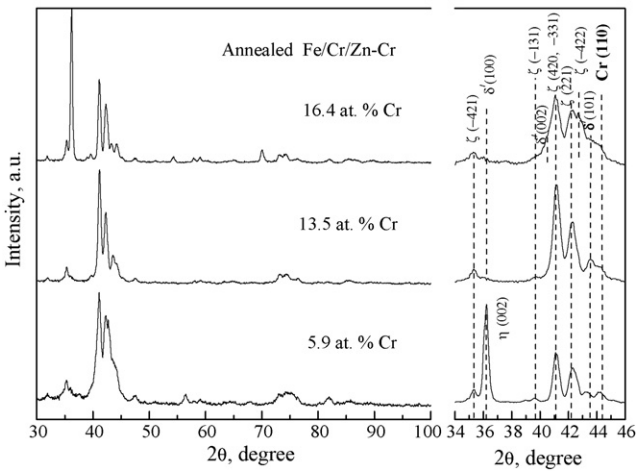

Fig. 4. XRD patterns of "annealed" Fe/Cr/Zn–Cr samples.

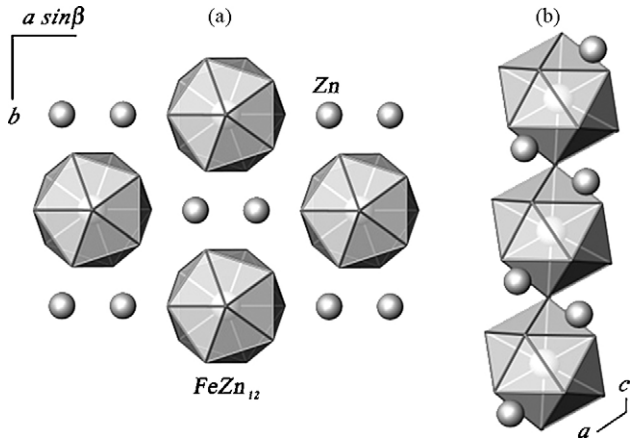

Fig. 5. Structure of ζ-$FeZn_{13}$. (a) Projection along *c*-axis; (b) projection along *b*-axis.

$c = 4.947$ Å; $V = 30.43$ Å^3. The axial ratio $c/a = 1.856$ deviates significantly from that of the ideal hexagonal close packing ($c/a = 1.633$). Some authors denote as η-phase Zn–Cr solid solutions which contain small amounts of Cr, up to 3 mass% [6]. According to other authors, this phase contains up to 8 mass% Cr (η-(Zn)) [15] or up to 15 mass% Cr (η-(Zn,Cr)) [15,22].

δ-(Zn,Cr)—Limited solid solutions of Cr in Zn–Cr_xZn_{1-x} ($0.03 < x < 0.20$), with hexagonal lattice, 2.732 Å $< a <$ 2.764 Å; 4.41 Å $< c <$ 4.49 Å. With increasing Cr content, the lattice parameter *a* of the solid solution increases, the parameter *c* decreases and the axial ratio *c*/*a* decreases systematically, reaching values close to that of the ideal hcp arrangement $c/a = 1.633$ [5,6,20].

Γ-(Zn,Cr)—Partially ordered limited solid solutions Cr_xZn_{1-x} ($0.2 < x < 0.4$); γ-brass type Cu_5Zn_8, cubic, space group I-43m (Nr. 217, PDF 71-0397). The crystal structure can be regarded as a superstructure resulting from the arrangement of 27 ($3 \times 3 \times 3$) partially vacated bcc α-type unit cells. In case of complete disorder, the XRD patterns contain lines of a body centered cubic sub-cell, space group Im-3m, type α-Cr with unit cell parameter 2.96 Å $< a <$ 3.02 Å [23].

ζ-(Zn,Cr)—A predominating phase formed only in the thermally treated Fe/Zn–Cr and Fe/Cr/Zn–Cr coatings. ζ-type intermetallides

Table 1
Phase composition (vol.%), unit cell parameters—*a*, *b*, *c* (Å), α, β, γ (°) and cell-volume—*V* (Å^3) for "as prepared"—(P) and "annealed"—(A) Fe/Zn,Cr and Fe/Cr/Zn–Cr galvanic coatings: (h) hexagonal, (m) monoclinic, (c) cubic.

As prepared (P)			Annealed (A)		
Phase composition	Relative content	Cell parameters and volume	Phase composition	Relative content	Cell parameters and volume
Fe/Zn,Cr (6.2 at.% Cr)					
δ-(Zn,Cr) (h)	100	$a = 2.718(2)$; $c = 4.619(2)$; $V = 29.55$	η-Zn (h)	23	$a = 2.665(2)$; $V = 30.38$; $c = 4.939(3)$
			ζ-(Zn,Cr) (m)	77	$a = 13.52(1)$; $b = 7.651(3)$; $c = 5.169(3)$; $\beta = 127.9°(4)$; $V = 421.9$
Fe/Zn,Cr (12.3 at.% Cr)					
δ-(Zn,Cr) (h)	93	$a = 2.748(2)$; $c = 4.492(3)$; $V = 29.38$	δ-(Zn,Cr) (h)	27	$a = 2.757(2)$; $V = 29.28$; $c = 4.448(3)$
Γ-(Zn,Cr) (c)	7	$a = 3.028(2)$; $V = 27.76$	ζ-(Zn,Cr) (m)	73	$a = 13.50(1)$; $b = 7.633(3)$; $c = 5.165(3)$; $\beta = 127.8°(5)$; $V = 420.5$
Fe/Zn,Cr (18.2 at.% Cr)					
δ-(Zn,Cr) (h)	69	$a = 2.757(2)$; $c = 4.450(2)$; $V = 29.29$	δ-(Zn,Cr) (h)	5	$a = 2.785(3)$; $V = 30.10$; $c = 4.482(3)$;
Γ-(Zn,Cr) (c)	31	$a = 3.018(2)$; $V = 27.49$	Γ-(Zn,Cr) (c)	5	$a = 3.018(2)$; $V = 27.49$
			ζ-(Zn,Cr) (m)	90	$a = 13.49(2)$; $b = 7.686(3)$; $c = 5.168(2)$; $\beta = 127.7°(5)$; $V = 423.9$
Fe/Cr/Zn,Cr (5.9 at.% Cr)					
δ-(Zn,Cr) (h)	100	$a = 2.720(1)$; $c = 4.662(3)$; $V = 29.87$	η-Zn (h)	24	$a = 2.664(2)$; $V = 30.35$; $b = 4.939(2)$;
			ζ-(Zn,Cr) (m)	76	$a = 13.50(1)$; $b = 7.673(3)$; $c = 5.169(2)$; $\beta = 128.0°$; $V = 424.0$
Fe/Cr/Zn,Cr (13.5 at.% Cr)					
δ-(Zn,Cr) (h)	73	$a = 2.719(2)$; $c = 4.667(2)$; $V = 29.88$	δ′-Zn,Cr) (h)	74	$a = 2.759(2)$; $V = 29.32$; $c = 4.448(2)$;
δ′-(Zn,Cr) (h)	27	$a = 2.757(1)$; $c = 4.448(2)$; $V = 29.29$	ζ-(Zn,Cr) (m)	26	$a = 13.54(2)$; $b = 7.647(2)$; $c = 5.173(2)$; $\beta = 127.9°$; $V = 422.7$
Fe/Cr/Zn,Cr (16.4 at.% Cr)					
δ-(Zn,Cr) (h)	35	$a = 2.719(1)$; $c = 4.667(2)$; $V = 29.88$	δ′-(Zn,Cr) (h)	16	$a = 2.767(1)$; $V = 29.50$; $c = 4.449(1)$;
δ′-(Zn,Cr) (h)	65	$a = 2.757(1)$; $c = 4.422(2)$; $V = 29.11$	ζ-(Zn,Cr) (m)	84	$a = 13.49(1)$; $b = 7.686(2)$; $c = 5.169(2)$; $\beta = 127.8°$; $V = 423.6$

Average for ζ-phase: $a = 13.510$ Å, $b = 7.663$ Å, $c = 5.169$ Å, $\beta = 127.83°$, $V = 423.4343$ Å^3 (present paper).
Original data of Scott: I2/m, $a = 10.93$ Å, $b = 7.68$ Å, $c = 5.11$ Å, $\beta = 100.76°$, $V = 421.40$ Å^3 [6].
Data of Scott transformed in C2/m: $a = 13.498$ Å, $b = 7.68$ Å, $c = 5.11$ Å, $\beta = 127.3°$, $V = 421.40$ Å^3.
$FeZn_{13}$(2): C2/m, $a = 13.424(5)$ Å, $b = 7.608(1)$ Å, $c = 5.061(3)$ Å, $\beta = 127.30(3)°$, $V = 411.16$ Å^3 [25].

of the general formula MZn_{13} (M = 7.14 at.%) have been isolated in the systems Ni–Zn, Fe–Zn, Co–Zn, and Mn–Zn [13]. They crystallize in the monoclinic space group C2/m. The structure of $FeZn_{13}$ is presented in Fig. 5. Iron atoms occupy special position (0, 0, ½) and are coordinated by 12 Zn atoms forming slightly deformed icosahedron (Fig. 5a). Neighboring icosahedral clusters are connected through a common Zn atom (special position (0, 0, 0)), in linear chains, running parallel to direction ⟨0 0 1⟩, (Fig. 5a). Adjacent chains are bridged by additional Zn atoms (Fig. 5b).

3.1. As deposited Fe/Zn–Cr and Fe/Cr/Zn–Cr coatings

Fe/Zn–Cr (6.2 at.% Cr): The XRD pattern for the as deposited coating is indexed with a hexagonal unit cell a = 2.718 Å; c = 4.619 Å (Table 1). The axial ratio c/a = 1.699 is rather close to that for ideal hcp structure (c/a = 1.633) than to pure Zn (c/a = 1.856). Unit cell parameters values and the relatively low content of Cr (x = 0.062) in the system allow assignment of this phase to the δ-(Zn,Cr) type solid solutions.

Fe/Zn–Cr (12.3 at.% Cr): The coating is bi-component. The major phase, 93 vol.%, is indexed with a hexagonal unit cell a = 2.748 Å; c = 4.492 Å; c/a = 1.635 (Table 1), values typical of δ-(Zn,Cr) phases [6]. The minor phase is indexed on the basis of a body centered cubic cell with parameter a = 3.028 Å, which suggests that it can be referred to the disordered Γ-(Zn,Cr) solid solutions. The content of Cr in this coating (12 at.%) is less than the lower concentration limit of Cr (≈20 at.%) at which the Γ-phase normally appears [20]. Since Zn–Cr alloy deposition is carried out at high current densities, reacting species are consumed rapidly at the cathode and the concentration in the vicinity of the cathode varies substantially as electrodeposition proceeds. From another point of view, due to the intense hydrogen evolution fast alkalization in the vicinity of the cathode takes place leading to transformation of the Cr(III) complexes—oligomerization, polymerization, etc. Under these conditions, the Cr concentration in the interface zone of the coating adjacent to the substrate may exceed the critical value of stability of the Γ-phase. It is worth noticing that a similar concentration profile has been observed in vacuum-evaporated Zn–Cr layers, where the concentration of Cr decreases from about 15 mass% near the substrate interface to about 5 mass% at the surface [6]. A gradient in the distribution of Cr, due to a change of Cr content in the Γ-phase and transition from bcc- to hcp-structure, from the interface substrate/coating zone towards the surface of Zn–Cr alloy coatings, electrodeposited from electrolytes without agitation is also established [24].

Fe/Zn–Cr (18.2 at.% Cr): The coating contains 69 vol.% δ-phase (a = 2.757 Å; c = 4.450 Å, c/a = 1.614) and 31 vol.% Γ-phase (a = 3.018 Å). These values of the unit cell parameters indicate higher content of Cr in both phases, compared to δ- and Γ-phases in sample Fe/Zn–Cr (12.3 at.% Cr).

Fe/Cr/Zn–Cr (5.9 at.% Cr): The phase composition of the coating deposited onto Cr protected substrate is practically identical to that of the non-protected Fe/Zn–Cr (6.2 at.% Cr). The XRD pattern exhibit peaks of δ-phase (a = 2.720 Å; c = 4.662 Å; c/a = 1.714) with a preferred orientation of ⟨0 0 1⟩ direction perpendicular to the sample plane, and as well peaks of α-Cr (4 vol.%), a = 2.883 Å. The peaks of α-Cr are probably due to diffraction from the substrate. No α-Fe lines were registered. The unit cell parameters and the axial ratio for the δ-phase do not differ substantially from those for the Fe/Zn–Cr (6.2 at.% Cr) sample, which has close elemental composition. It can be concluded, therefore, that the coating is a single-phase δ-(Zn,Cr) solid solution.

Fe/Cr/Zn–Cr (13.5 at.% Cr): The XRD pattern of the coating exhibit lines of two hexagonal phases, δ-(Zn,Cr) type, that is why the symbol δ′ is also used. The lattice parameters of the δ-phase (a = 2.719 Å; c = 4.667 Å; c/a = 1.716) are practically identical to those of Fe/Cr/Zn–Cr (5.9 at.% Cr). The parameters of the δ′-phase (a = 2.757 Å; c = 4.448 Å; c/a = 1.613), correspond to those observed for the δ-phases with increased Cr content (Fe/Zn–Cr (18.2 at.% Cr)). Both phases exhibit preferred orientation of the ⟨0 0 1⟩ direction perpendicular to the sample surface. The δ′-phase with lower axial ratio (c/a = 1.613) has probably formed at the beginning of the deposition process, at higher relative concentrations of electroactive Cr(III) species in the in the vicinity of the electrode. The δ-phase has higher axial ratio (c/a = 1.713), i.e. lower Cr content, and seems to be deposited at a later stage of the deposition process. Traces of α-Cr are also observed. Γ-type phases were not detected.

Fe/Cr/Zn–Cr (16.4 at.% Cr): Like the previous sample, the coating contains two hexagonal phases, assigned as: δ (a = 2.719 Å; c = 4.667 Å; c/a = 1.716), with sharp symmetric diffraction lines and preferred orientation of the ⟨0 0 1⟩ direction perpendicular to the substrate surface, and δ′ (a = 2.757 Å; c = 4.422 Å; c/a = 1.604), a phase with no preferred orientation and broad asymmetric XRD lines. The unit cell parameter values and the diffraction line profiles indicate that δ′-phase has higher Cr content and is probably formed at the beginning of the deposition process. The content of Cr in δ-phase is lower. The observed broadening and asymmetry of the X-ray diffraction lines could be due to presence of Cr concentration profile (decrease of Cr content in direction from substrate/coating interface to external coating surface).

3.2. Annealed Fe/Zn–Cr and Fe/Cr/Zn–Cr coatings

Fe/Zn–Cr (6.2 at.% Cr) A: The basic components of the coating, after thermal treatment of the sample, are: ζ-phase, monoclinic, space group C2/m, (a = 13.52 Å; b = 7.651 Å; c = 5.169 Å; β = 127.9°) and η-Zn, space group $P6_3/mmc$, (a = 2.665 Å; c = 4.939 Å; c/a = 1.853). The lattice parameters of η-phase practically match those of pure Zn. Theoretically, the content of the 3-d transition metal M in ζ-MZn_{13} intermetallides, derived from the content of their unit cell, is 7.14 at.%. If we assume that the segregated η-phase is pure Zn, then from the nominal atomic composition of coating it follows that the content of Cr in the ζ-phase is ≈8 at.%, i.e. the observed ζ-phase is $CrZn_{13}$. The thermally induced transformation δ-(Zn,Cr) → ζ-(Zn,Cr) is irreversible [6].

Fe/Zn–Cr (12.3 at.% Cr) A: The basic component of this coating after thermal treatment is ζ-phase (a = 13.50 Å; b = 7.633 Å; c = 5.165 Å; β = 127.8°). The content of the hexagonal δ-phase (a = 2.757 Å; c = 4.448 Å; c/a = 1.613), is considerably lower. The lattice parameters of the ζ-phase do not differ substantially from those observed for the previous sample. The parameters of the δ-phase, however, have values typical for relatively rich in Cr hexagonal phases. If we assume that the observed ζ-phase is indeed $CrZn_{13}$, then judging by the volume content of the ζ- and δ-phases and the nominal atomic composition of the coating, we can conclude that the composition of δ-phase is $Cr_{0.26}Zn_{0.74}$, (22 mass% Cr content).

Fe/Zn–Cr (18.2 at.% Cr) A: Thermal treatment of this coating results in almost complete transformation of the δ- and Γ-phases into ζ-phase. A multiple-phase coating is obtained in which ζ-phase (a = 13.49 Å; b = 7.686 Å; c = 5.168 Å; β = 127.7°) is the major component. δ-phase (a = 2.785 Å; c = 4.482 Å; c/a = 1.609) and Γ-phase (a = 3.018 Å) are residual.

Fe/Cr/Zn–Cr (5.9 at.% Cr) A: The basic components of the coating are: ζ-phase (a = 13.50 Å; b = 7.673 Å; c = 5.169 Å; β = 128.0°) and η-Zn (a = 2.664 Å; c = 4.939 Å; c/a = 1.854).

Fe/Cr/Zn–Cr (13.5 at.% Cr) A: This is a multi-phase coating with basic components: ζ-phase (a = 13.54 Å; b = 7.647 Å; c = 5.173 Å; β = 127.9°) and δ′-phase (a = 2.759 Å; c = 4.448 Å; c/a = 1.612). Weak lines of Cr are observed as well. The δ′-phase is most probably non-decomposed δ′-phase detected in the starting sample Fe/Cr/Zn–Cr (13.5 at.% Cr).

Fe/Cr/Zn–Cr (16.4 at.% Cr) A: This is a multi-phase coating with basic components: ζ-phase (a = 13.49 Å; b = 7.686 Å; c = 5.169 Å; β = 127.8°) and δ′-phase (a = 2.767 Å; c = 4.449 Å; c/a = 1.608). Weak lines for Cr are also observed. The δ′-phase is most probably residual δ′-phase detected in Fe/Cr/Zn–Cr (16.4 at.% Cr).

Summarized XRD data for the "as prepared" and "annealed" Zn–Cr coatings allow deducing some empirical trends in the dependence of phase composition and stability on nominal elemental composition and conditions of preparation. "As prepared" coatings having nominal Cr content between 6 and 18 at.%, consist of non-equilibrium (non-existing in the equilibrium-phase diagram) δ-(Zn,Cr) and Γ-(Zn,Cr) phases [6,7]. The δ-phase can be regarded as super-saturated solid solution of Cr in Zn matrix. In the crystal structure of the latter, each Zn atom has six lateral nearest neighbors at distance of about 2.66 Å and another six, more distant, at about 2.91 Å. The random substitution of Cr for Zn introduces positional disorder in the system leading to gradual equalization of all 12 distances. With increasing nominal Cr content, the parameter (a) of the hexagonal δ-phase increases, the parameter (c) decreases and the axial ratio c/a tends to 1.633.

The Γ-(Zn,Cr) appears as disordered Cu_5Zn_8 γ-brass type phase whose diffraction pattern contain lines of bcc lattice, 3.018 Å < a < 3.028 Å. For the particular samples studied, the variation of unit cell parameter is not markedly pronounced. However, our previous studies of Zn–Cr coatings, obtained at different electrochemical conditions, have shown that a decreases almost linearly with increasing Cr in a wide concentration range [25,26].

The atomic percentage of Cr (x_{Cr}) in δ-(Zn,Cr) and Γ-(Zn,Cr) could be evaluated roughly without any theoretical implications, assuming that the unit cell volume V_p of a given Zn–Cr phase varies linearly with x_{Cr}, between unite cell volumes of the pure bcc Cr (V_{Cr} = 24.01 Å^3) and that of pure hcp Zn (V_{Zn} = 30.43 Å^3). Please, have in mind that the hexagonal Zn and the cubic α-Cr contain two metal atoms in their unit cells:

$$V_p = x_{Cr}V_{Cr} + (1 - x_{Cr})V_{Zn}; \quad \text{or} \quad x_{Cr} = \frac{30.43 - V_p}{6.42} \tag{1}$$

The atomic percentage $(x_{Cr})_\delta$ and $(x_{Cr})_\Gamma$ of Cr calculated for δ- and Γ-(Zn,Cr) phases using Eq. (1) and unit cell volume data given in Table 1, falls in the intervals 9 at.% < $(x_{Cr})_\delta$ < 21 at.% and 41 at.% < $(x_{Cr})_\Gamma$ < 45 at.%. These results do not differ essentially from existing data.

The δ-phase is the major constituent of "as prepared" Fe/Zn–Cr coatings, deposited on unprotected substrate (Table 1). At higher Cr content it is accompanied by Γ-phase, whose amount increases with increasing Cr content. In contrast to Fe/Zn–Cr the Cr-protected (Fe/Cr/Zn–Cr) coatings consist exclusively of δ-phases. This characteristic may arise from different electrochemical conditions at the surface of non-plated steel and Cr-plated steel electrode. It may be as well due to the fact that the electrolyte at the surface of the unprotected electrode is contaminated with Fe. Finally, the Cr concentration profile for coatings deposited on non-protected electrodes may be much steeper, than that for protected electrodes. In such a case, the local concentration of Cr could be large enough to fall within the compositional interval of existence of Γ-phase. So far, this effect remains open for discussion.

The "annealed" coatings are multiphase. The major constituent—the equilibrium ζ-phase is accompanied by intermediate amounts of η- or δ-phases and minor amounts of Γ-phase. The phase composition is related to the Cr content in the "as prepared" coatings. On annealing, the equilibrium ζ-$CrZn_{13}$ phase (7.14 at.% Cr) precipitates from the non-equilibrium δ-phase in the "as prepared" coatings. With Cr content less than 7.14 at.% the δ-phase decomposes to ζ-$CrZn_{13}$ and pure η-Zn. When the Cr atomic percentage is greater than 7.14, the Cr is distributed between the ζ- and δ- or Γ-phases. Precipitation of ζ-(Zn,Cr) phases on annealing of supersaturated δ-(Zn,Cr) solid solutions has also been reported by Hashimoto et al. for electrodeposited Zn–Cr alloy coatings of more than 5.7 mass% Cr, subjected to thermal treatment [18,19]. The question that still requires answer is: Are the precipitated ζ-phases contaminated with Fe from the substrate?

The unit cell parameters for ζ-phases, summarized in Table 1, agree well with those reported by Scott et al. for evaporated and annealed thin Zn–Cr films [6]: standard C2/m setting, a = 13.498 Å; b = 7.68 Å; c = 5.11 Å; β = 127.3°; V = 421.40 Å^3. It should be noted that the original setting used by Scott *et al.* is I2/m: a = 10.93 Å; b = 7.68 Å; c = 5.11 Å; β = 100.76°; V = 421.40 Å^3. As seen from Table 1, deviations from average values of the cell parameters and volumes are small and random. This is valid not only for the ζ-phases formed in the coatings with different Cr content, but as well for the coatings on protected and non-protected substrates. The average unit cell parameters and volume (a = 13.51 Å; b = 7.663 Å; c = 5.169 Å; β = 127.9°; V = 423.43 Å^3) are much higher than those for $FeZn_{13}$ (a = 13.424 Å; b = 7.608 Å; c = 5.061 Å; β = 127.30°; V = 411.16 Å^3) [27]. This is due to the fact that the atomic radius of Cr (1.304 Å) is larger than that of Fe (1.274 Å). Hence, judging by the values of the obtained lattice parameters and the similarities in phase composition of annealed coatings on protected and non-protected substrates it can be concluded that if Fe is partly substituted for Cr at the center of the icosahedral cluster, its relative amount should not exceed few tenths of a percent.

4. Conclusions

Zn–Cr alloy coatings with Cr content between 6 and 18 at.% were obtained in a flow cell in order to reach the working conditions of the high speed electrodeposition on steel strips. The "as prepared" coatings consist of non-equilibrium δ-(Zn,Cr) (super-saturated solid solution of Cr in Zn matrix) and Γ-(Zn,Cr) (disordered Cu_5Zn_8 γ-brass type) phases. The coatings with low Cr content are single δ-(Zn,Cr) phase. At higher Cr content, on non-protected steel substrates δ-phase is accompanied by Γ-phase, whose amount increases with the Cr content, while on Cr-protected steel two δ-phases, with different Cr content co-exist.

The "annealed" coatings consist exclusively of ζ-$CrZn_{13}$ equilibrium phase. The phase composition is related to that of the "as prepared" coatings. When Cr content is less than 7.14 at.% the δ-phase decomposes to ζ- and pure η-Zn. When the atomic percentage is grater than 7.14, the Cr is distributed between the ζ- and δ- or Γ-phases.

The values of the obtained lattice parameters and the similarities in phase composition of annealed coatings on protected and non-protected steel substrates evidences that the iron from the substrates does not contaminate substantially the ζ-$CrZn_{13}$ phase.

The effect of the annealing conditions (temperature, annealing time) on phase composition will be a subject of further study as well as the properties of the ζ-$CrZn_{13}$ phase.

Acknowledgement

The investigations have been performed with the support of FFG and Land Niederösterreich in the frame of the COMET-program.

References

[1] Y. Miyoshi, H. Odashima, Y. Shindo, M. Yoshida, T. Kamanaru, Nippon Steel Technical Report No. 57, 16–21 April 1993, pp. 16–21.
[2] T. Ichida, Galvatech'95 Conference Proceedings, Iron and Steel Society, Chicago, 1995, pp. 359–369.
[3] L. Guzman, M. Adami, W. Gissler, S. Klose, S. De Rossi, Surf. Coat. Technol. 125 (2000) 218–222.
[4] US Patent 5,510,196 (1996).
[5] US Patent 6,682,828 B2 (2004).

[6] C. Scott, C. Olier, A. Lamande, P. Choquet, D. Chaleix, Thin Solid Films 436 (2003) 232–237.
[7] M. Hansen, E. Anderko, Constitution of Binary Alloys, Metallurgizdat, Moscow, 1962.
[8] H. Hanemann, Z. Metallkd. 32 (1940) 91–92.
[9] Z. Moser, L.A. Heldt, J. Phase Equilib. 13 (2) (1992) 172–176.
[10] G. Reumont, P. Perrot, J. Phase Equilib. 24 (1) (2003) 50–54.
[11] N.-Y. Tang, X.B. Yu, J. Phase Equilib. Diffus. 26 (1) (2005) 50–54.
[12] H. Hartmann, W. Hofmann, D. Müller, Abhandl. Braunschweig. Wiss. Ges. 7 (1955) 100–106.
[13] P.J. Brown, Acta Cryst. 15 (1962) 608–612.
[14] G. Reumont, S. Maniez, B. Gay, P. Perrot, J. Mater. Sci. Lett. 19 (2000) 2081–2084.
[15] US Patents 4,877,494 (1989), 4,897,317 (1990).
[16] A. Takahashi, Y. Miyoshi, T. Hada, J. Electrochem. Soc. 141 (1994) 954–957.
[17] M. El-Sharif, C. Chisholm, Y. Sut, L. Feng, Advances in Surface Engineering, 1, vol. 206, Royal Society of Chemistry, 1997, pp. 95–110.
[18] S. Hashimoto, S. Ando, T. Urakawa, M. Sagiyama, J. Japan Inst. Met. 52 (1) (1998) 9–14.
[19] S. Hashimoto, M. Nagoshi, S. Ando, T. Urakawa, M. Sagiyama, GALVATECH'98, Chiba, Japan, 1998, pp. 537–541.
[20] M. Miyake, T. Hirato, E. Matsubara, Y. Awakura, Second International Conference on Processing Materials for Properties, San Francisco, CA, November 5–8, 2000, pp. 779–782.
[21] W. Kraus, G. Nolze, PowderCell for Windows, version 2.4, Federal Institute for Materials Research and Testing, Rudower Chaussee 5, 12489 Berlin, Germany, 2000.
[22] US Patent 4,877,494 (1989), EP 0285931 A1 (1988), US Patent 4,897,317 (1990).
[23] J.K. Brandon, R.Y. Brizard, P.C. Chieh, R.K. McMillan, W.B. Pearson, Acta Cryst. B 30 (1974) 1412–1417.
[24] Tz. Boiadjieva, D. Kovacheva, L. Lyutov, M. Monev, J. Appl. Electrochem. 38 (2008) 1435–1443.
[25] Tz. Boiadjieva, D. Kovacheva, K. Petrov, S. Hardcastle, A. Sklyarov, M. Monev, J. Appl. Electrochem. 34 (2004) 315–321.
[26] Tz. Boiadjieva, D. Kovacheva, K. Petrov, S. Hardcastle, M. Monev, Corr. Sci. 46 (2004) 681–695.
[27] C. Belin, M. Tillard, L. Monconduit, Acta Cryst. C 56 (2000) 267–268.